

Stepwise Reversible Oxidation of *N*-Peralkyl-Substituted NHC–CAAC Derived Triazaalkenes: Isolation of Radical Cations and Dications

Debdeep Mandal,[†] Ramapada Dolai,[†] Nicolas Chrysochos,[‡] Pankaj Kalita,[§] Ravi Kumar,[⊥] Debabrata Dhara,[†] Avijit Maiti,[†] Ramakirushnan Suriya Narayanan,[†] Gopalan Rajaraman,^{*,⊥,||} Carola Schulzke,^{*,‡} Vadapalli Chandrasekhar,^{*,†,||} and Anukul Jana^{*,†,||}

[†]TIFR Centre for Interdisciplinary Sciences Hyderabad, 21, Brundavan Colony, Narsingi, Hyderabad 500075, India

[‡]Institut für Biochemie, Ernst-Moritz-Arndt Universität Greifswald, Felix-Hausdorff-Straße 4, D-17487 Greifswald, Germany

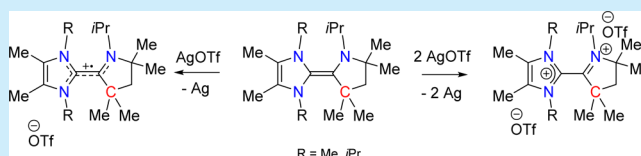
[§]School of Chemical Sciences, National Institute of Science Education and Research, Bhubaneswar 752050, Odisha, India

[⊥]Department of Chemistry, Indian Institute of Technology Bombay, Powai, Mumbai 400076, India

^{||}Department of Chemistry, Indian Institute of Technology Kanpur, Kanpur 208016, India

S Supporting Information

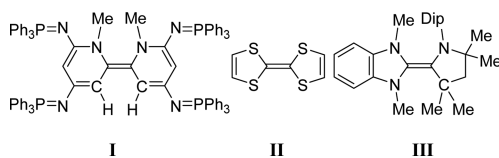
ABSTRACT: Herein, the isolation and characterization of *N*-peralkyl-substituted NHC–CAAC derived triazaalkenes in three oxidation states, neutral, radical cation, and dication, are reported. Cyclic voltammetry has shown the reversible electronic coupling between the first and second oxidation to be $\Delta E_{1/2} = 0.50$ V. As a proof-of-principle, to demonstrate the electron-rich nature of the triazaalkene, it was shown that it



it can be used as an electron donor in the reduction of an aryldiazonium salt to the corresponding arene.

In recent years, electron-rich alkenes such as **I** (Scheme 1) have caught the imagination of the research community,

Scheme 1. Chemical Structures of an Electron-Rich Olefin I, Tetrathiofulvalene II, and NHC–CAAC Heterodimer III (Dip = 2,6-*i*Pr₂C₆H₃)



particularly in view of their potential applications as electron donors in organic reactions.¹ However, in contrast to the classical example of tetrathiofulvalene (TTF), **II**² (Scheme 1), with many other electron-rich olefins, it has not been possible to isolate radical cations.³ In view of the potential applications demonstrated by the tetrathiofulvalene family of compounds in diverse research fields,⁴ including electronic devices,⁵ it is of interest to explore whether other families of electron-rich olefins can be prepared with similar or larger electronic coupling between their first and second oxidation events. If realized, one can expect the isolation of redox-amphoteric radical cations and their subsequent use in various applications.⁶ Cyclic alkyl amino carbene (CAAC) ligands⁷ appear to be extremely suitable for stabilizing C-center based radicals⁸ and other entities possessing reactive functionalities.⁹ Bertrand and co-workers have recently reported the isolation of a NHC–CAAC heterodimer, **III**

(Scheme 1), possessing three stable oxidation states, utilizing two different motifs: a benzannulated backbone functionalized *N*-methyl-substituted NHC and a *N*-aryl-substituted CAAC.¹⁰

One of the important features of NHCs has been their sensitivity to the substituents present, either in the backbone or on nitrogen. Indeed, remarkable differences in reactivities of NHCs have been observed in organocatalysis¹¹ and in main-group organometallic chemistry¹² upon variation in the ligand backbone (e.g., saturated, unsaturated, benzannulated) and *N*-substituents (aryl¹³ vs alkyl¹⁴) as a result of the modulation of the stereoelectronic factors. Given this background in NHC chemistry, it is surprising that the reported chemistry of CAAC, thus far, is confined to only *N*-aryl substitution¹⁵ except for a single report describing the synthesis of a *N*-*t*Bu-substituted CAAC as its lithium triflate adduct.¹⁶ This has motivated us to study the *N*-alkyl-substituted CAAC system, which is reported herein.

We have considered the Me group as the backbone of unsaturated *N*-alkyl-substituted NHC **1**^{Me} and **1**^{iPr} along with *N*-isopropyl-substituted cyclic iminium salt **2**^{iPr} as the building blocks, with the anticipation that the NHC will attack the electrophilic carbon center of the cyclic iminium salt, leading to the conjugate acids of NHC–CAAC derived alkenes.^{10,17} A similar strategy was used for the dimerization of diaminocarbenes to obtain tetraazaalkenes.¹⁸ Accordingly, **1**^{Me} and **1**^{iPr} were reacted separately with **2**^{iPr}¹⁹ in THF at rt, leading to the

Received: September 2, 2017

formation of the conjugated acids of triazaolefins, **3**^{MeiPr} (93%) and **3**^{iPriPr} (91%) as colorless solids (Scheme 2).¹⁹

Scheme 2. Syntheses of **3**



The ¹H NMR spectra of compounds **3**^{MeiPr} (δ = 4.48 ppm) and **3**^{iPriPr} (δ = 4.70 ppm) reveal a characteristic singlet for the “C–H” unit. These chemical shifts are considerably upfield shifted when compared with that of the starting cyclic iminium salt **2**^{iPr} (δ = 9.23 ppm).

The solid-state molecular structures of **3**^{MeiPr} and **3**^{iPriPr}¹⁹ were confirmed by single-crystal X-ray diffraction studies (Figure 1),

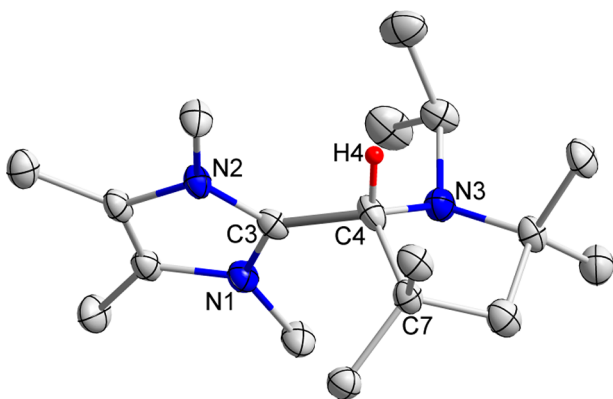
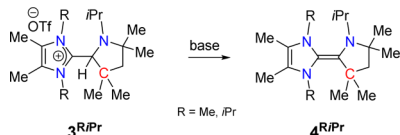


Figure 1. Molecular structure of **3**^{MeiPr} in the solid state (thermal ellipsoids at 50%, triflate anion, and H atoms except C4–H omitted for clarity). Selected bond lengths (Å) and angles (°): C3–C4 1.517(3); N2–C3–N1 107.2(2), N3–C4–C7 105.8(2).

which are consistent with their solution behavior. The bond distances between the connecting carbon centers of the two heterocycles are 1.517(3) and 1.510(3) Å, respectively, for **3**^{MeiPr} and **3**^{iPriPr}.

Subsequent deprotonation of **3**^{MeiPr} and **3**^{iPriPr} with potassium bis(trimethylsilyl)amide (KN(TMS)₂) and lithium-2,2,6,6-tetramethylpiperidine (LiTMP) afforded **4**^{MeiPr} (92%) and **4**^{iPriPr}

Scheme 3. Syntheses of **4**

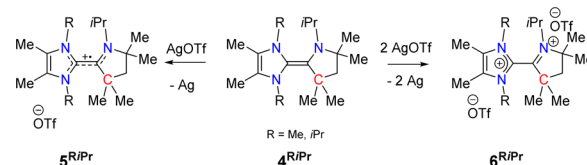


(46%), respectively (Scheme 3).¹⁹ Solution-state ¹H and ¹³C{¹H} NMR spectra of **4**^{MeiPr} and **4**^{iPriPr} are consistent with their expected chemical structures; both are stable in solution under inert atmosphere, and we did not observe any kind of change even up to 80 °C.

The cyclic voltammogram of **4**^{MeiPr} showed two reversible one-electron redox processes with an electronic coupling of $\Delta[E_{1/2}(\mathbf{4}^{\text{MeiPr}})] = 0.50$ V at –20 °C,¹⁹ which is larger than that of **II** ($\Delta[E_{1/2}] = 0.37$ V)²⁰ and **III** ($\Delta[E_{1/2}] = 0.34$ V).¹⁰

Encouraged by the electrochemical studies and with a desire to isolate the oxidized products, we reacted **4**^{MeiPr} and **4**^{iPriPr} with AgOTf in a 1:1 and 1:2 ratio, respectively (Scheme 4).¹⁹ In the

Scheme 4. Syntheses of **5** and **6**



case of the 1:1 reaction, we observed an immediate visible color change from colorless to deep orange red, and we isolated the corresponding radical cations **5**^{MeiPr} (86%) and **5**^{iPriPr} (70%).

X-band EPR measurement of **5**^{MeiPr} and **5**^{iPriPr} in THF solution at rt shows that the unpaired electron in these compounds is coupled with all three nitrogen atoms, as indicated by the presence of hyperfine coupling in the EPR spectra (Figure 2).¹⁹

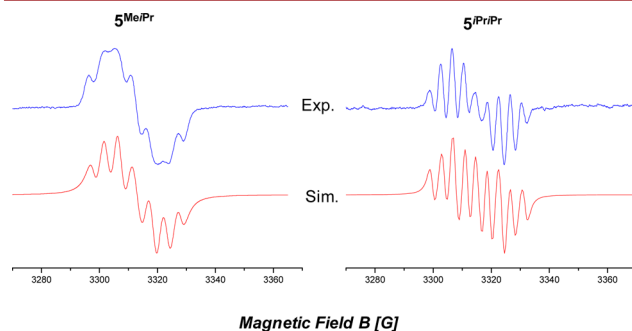


Figure 2. Experimental and simulated EPR spectra of **5**^{MeiPr} and **5**^{iPriPr} in THF.

Simulation of the EPR spectra yielded 16.8, 13.2, and 12.0 MHz and 19.8, 12.7, and 10.4 MHz as the hyperfine coupling constants involving the three nitrogen atoms in **5**^{MeiPr} and **5**^{iPriPr}, respectively.²¹ For both compounds, an isotropic *g* tensor of 2.006 was estimated. One large and two smaller isotropic hyperfine constants are noted in both cases, which clearly suggests that the spin density is delocalized from the carbon atom to all three nitrogen atoms. We have also estimated the *g* and hyperfine tensors of these compounds using DFT methods employing the ORCA suite of programs,²² affording values 14.3, 14.2, and 10.7 MHz (**5**^{MeiPr}) and 14.1, 14.1, and 7.7 MHz (**5**^{iPriPr}) for N₁, N₂, and N₃, respectively. These estimated values are consistent with the simulations, and the differences in the hyperfine coupling are found to arise from the spin-dipolar term.

Radical cations of **5**^{MeiPr} and **5**^{iPriPr} showed absorption in the UV/vis region, whereas the parent alkenes **4**^{MeiPr} and **4**^{iPriPr} show absorption only in the UV region. In the UV/vis spectra, **5**^{MeiPr} shows two absorption bands at $\lambda_{\text{max}}(\epsilon) = 379$ (1399.0) and 452 (349.4) nm (L mol^{–1} cm^{–1}), whereas **5**^{iPriPr} exhibits three absorption bands at $\lambda_{\text{max}}(\epsilon) = 280$ (1556.8), 371 (1913.2), and 465 (494.7) nm (L mol^{–1} cm^{–1}). These values are blue-shifted when compared with **III** ($\lambda_{\text{max}}(\epsilon) = 530$ nm). TD-DFT calculations show that the longest wavelength absorptions of **5**^{MeiPr} at 452 nm and of **5**^{iPriPr} at 465 nm correspond to the transition of an α -spin of the SOMO (singly occupied molecular orbital) to an α -spin of the LUMO. Adjacent transitions at 379 and 371 nm in **5**^{MeiPr} and **5**^{iPriPr}, respectively, correspond to a β -spin of HOMO to β -spin of LUMO transition.¹⁹ In case of **5**^{iPriPr},

the signal at 280 nm is due to the transition of an α -spin of the SOMO to an α -spin of the LUMO+1.¹⁹

Solid-state structure analysis of 5^{MeiPr} and 5^{iPrPr} shows that the central C–C bond lengths are 1.484(3) and 1.444(8) Å, respectively (Figure 3). These are longer than standard C–C

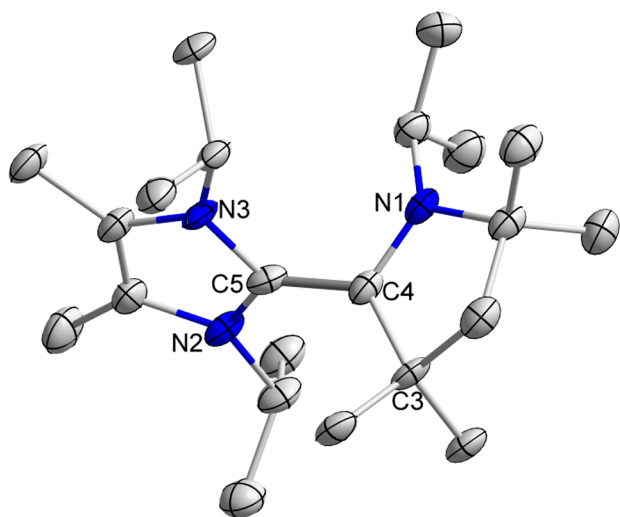


Figure 3. Molecular structure of 5^{iPrPr} in the solid state (thermal ellipsoids at 30%, triflate anion, and H atoms omitted for clarity). Selected bond lengths (Å) and angles ($^{\circ}$): C4–C5 1.444(8); N1–C4–C3 111.4(5), N2–C5–N3 106.6(5).

double bond lengths, suggesting that the oxidized products are formed by the removal of an electron from the bonding orbital. The torsion angles between the two heterocycles of 5^{MeiPr} and 5^{iPrPr} are 73.77 and 57.73 $^{\circ}$, respectively. The differences in these angles presumably arise due to the steric differences between the Me and $^{\text{iPr}}$ groups on the N-centers of the NHC moiety. The sum of the bond angles around the N-centers of the CAAC moiety of 5^{MeiPr} and 5^{iPrPr} is 344.86 and 356.30 $^{\circ}$, respectively, indicating some degree of pyramidalized geometry, which is quite unlike what is found in NHCs.

In the 1:2 reaction of 4^{MeiPr} and 4^{iPrPr} with AgOTf, we obtained corresponding dications 6^{MeiPr} and 6^{iPrPr} in good yields. Analysis of solid-state molecular structures of 6^{MeiPr} and 6^{iPrPr} reveal that upon oxidation of the radical cation to the dication the central C–C bond length is almost unchanged (5^{MeiPr} (1.484(3) Å) to 6^{MeiPr} (1.482(2) Å) and 5^{iPrPr} (1.444(8) Å) to 6^{iPrPr} (1.487(5) Å) (Figure 4). The torsion angles between the two heterocycles of the dications 6^{MeiPr} and 6^{iPrPr} are 89.59 and 88.48 $^{\circ}$, which are very close to each other.

After the isolation of three oxidation states of NHC–CAAC derived alkenes, we carried out stoichiometric reactions between neutral and dicationic NHC–CAAC heterodimers (Scheme 5).¹⁹ The formation of the radical cations in this comproportionation reaction is another strong indication, in addition to cyclic voltammetry results, of the reversible nature of the electron transfer.

Finally, to demonstrate the reductant properties of the newly synthesized electron-rich olefins, we considered the reduction of 4-methoxybenzenediazonium tetrafluoroborate, **7** with 4^{MeiPr} . At rt, involving a 1:1 reaction, the formation of anisole **8** under elimination of N_2 gas was indeed detected (Scheme 6).¹⁹ We have not attempted to optimize the reaction conditions, though the electron donor capability of 4^{MeiPr} has been established.

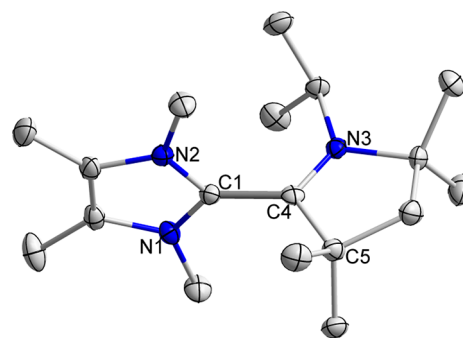
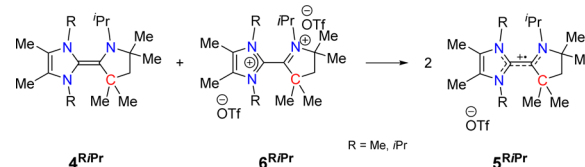
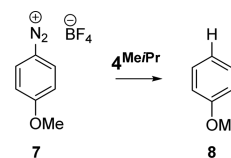


Figure 4. Molecular structure of 6^{MeiPr} in the solid state (thermal ellipsoids at 30%, triflate anion, and H atoms omitted for clarity). Selected bond lengths (Å) and angles ($^{\circ}$): C1–C4 1.482(2); N1–C1–N2 108.15(13), N3–C4–C5 113.44(14).

Scheme 5. Comproportionation of **4** and **6** to **5**



Scheme 6. Reduction of **7** by 4^{MeiPr}



In summary, we have disclosed *N*-peralkyl-substituted NHC–CAAC derived electron-rich triazaolefins, which exhibit three stable oxidation states with $\Delta E_{1/2} = 0.50$ V, larger than that of TTF and therefore showing potential for future applications. The reversible nature of the electron transfer process was demonstrated both electrochemically as well as chemically (comproportionation reaction). Currently, we are extending the scope of these studies to prepare a larger variety of such compounds and also to explore their properties further.

■ ASSOCIATED CONTENT

Supporting Information

The Supporting Information is available free of charge on the ACS Publications website at DOI: 10.1021/acs.orglett.7b02721.

Experimental and computational details (PDF)
Crystallographic details and data (CIF)

■ AUTHOR INFORMATION

Corresponding Authors

*E-mail: rajaraman@chem.iitb.ac.in.
*E-mail: carola.schulzke@uni-greifswald.de.
*E-mail: vc@tifrh.res.in.
*E-mail: ajana@tifrh.res.in.

ORCID

Gopalan Rajaraman: 0000-0001-6133-3026
Vadapalli Chandrasekhar: 0000-0003-1968-2980
Anukul Jana: 0000-0002-1657-1321

Notes

The authors declare no competing financial interest.

■ ACKNOWLEDGMENTS

This work is supported by the TIFR Centre for Interdisciplinary Science Hyderabad, Hyderabad, India, and SERB-DST (EMR/2014/001237), India. V.C. is thankful to the Department of Science and Technology, New Delhi, India, for a National J.C. Bose fellowship. G.R. would like to thank SERB-DST EMR/2014/000247 for funding. We are indebted to Prof. Ranjan Das, TIFR Mumbai, India, for the measurement of EPR. We are thankful to Prof. David Scheschkewitz, Saarland University, Saarbrücken, Germany, for getting the measurement of elemental analysis. We are also thankful to Dr. Sanjib Patra, IIT Kharagpur, India, for the single-crystal X-ray data of 2^{IPr} and 3^{MeiPr} , and Dr. Rahul Bannerjee, NCL Pune, India, for the single-crystal X-ray data of 6^{MeiPr} .

■ REFERENCES

- (1) For selected references: (a) Barham, J. P.; Coulthard, G.; Kane, R. G.; Delgado, N.; John, M. P.; Murphy, J. A. *Angew. Chem., Int. Ed.* **2016**, *55*, 4492–4496. (b) Hanson, S. S.; Doni, E.; Traboulsee, K. T.; Coulthard, G.; Murphy, J. A.; Dyker, C. A. *Angew. Chem., Int. Ed.* **2015**, *54*, 11236–11239. (c) Broggi, J.; Terme, T.; Vanelle, P. *Angew. Chem., Int. Ed.* **2014**, *53*, 384–413. (d) Zhou, S.; Anderson, G. M.; Mondal, B.; Doni, E.; Ironmonger, V.; Kranz, M.; Tuttle, T.; Murphy, J. A. *Chem. Sci.* **2014**, *5*, 476–482. (e) Doni, E.; Murphy, J. A. *Chem. Commun.* **2014**, *50*, 6073–6087. (f) Doni, E.; Mondal, B.; O'Sullivan, S.; Tuttle, T.; Murphy, J. A. *J. Am. Chem. Soc.* **2013**, *135*, 10934–10937.
- (2) Wudl, F.; Smith, G. M.; Hufnagel, E. J. *J. Chem. Soc. D* **1970**, 1453–1454.
- (3) (a) Murphy, J. A.; Garnier, J.; Park, S. R.; Schoenebeck, F.; Zhou, S.; Turner, A. T. *Org. Lett.* **2008**, *10*, 1227–1230. (b) Ames, J. R.; Houghtaling, M. A.; Terrian, D. L.; Mitchell, T. A. *Can. J. Chem.* **1997**, *75*, 28–36.
- (4) For selected references: (a) Bergkamp, J. J.; Decurtins, S.; Liu, S.-X. *Chem. Soc. Rev.* **2015**, *44*, 863–874. (b) Goetz, K. P.; Vermeulen, D.; Payne, M. E.; Kloc, C.; McNeil, L. E.; Jurchescu, O. D. *J. Mater. Chem. C* **2014**, *2*, 3065–3076. (c) Rovira, C. *Chem. Rev.* **2004**, *104*, 5289–5317.
- (5) Alves, H.; Molinari, A. S.; Xie, H.; Morpurgo, A. F. *Nat. Mater.* **2008**, *7*, 574–580.
- (6) Lorcy, D.; Bellec, N. *Chem. Rev.* **2004**, *104*, 5185–5202.
- (7) Lavallo, V.; Canac, Y.; Präsang, C.; Donnadiou, B.; Bertrand, G. *Angew. Chem., Int. Ed.* **2005**, *44*, 5705–5709.
- (8) For selected references: (a) Mondal, K. C.; Roesky, H. W.; Schwarzer, M. C.; Frenking, G.; Tkach, I.; Wolf, H.; Kratzert, D.; Herbst-Irmer, R.; Niepötter, B.; Stalke, D. *Angew. Chem., Int. Ed.* **2013**, *52*, 1801–1805. (b) Mahoney, J. K.; Martin, D.; Moore, C. E.; Rheingold, A. L.; Bertrand, G. *J. Am. Chem. Soc.* **2013**, *135*, 18766–18769. (c) Mahoney, J. K.; Martin, D.; Thomas, F.; Moore, C. E.; Rheingold, A. L.; Bertrand, G. *J. Am. Chem. Soc.* **2015**, *137*, 7519–7525.
- (9) For selected references: (a) Kinjo, R.; Donnadiou, B.; Celik, M. A.; Frenking, G.; Bertrand, G. *Science* **2011**, *333*, 610–613. (b) Ung, G.; Rittle, J.; Soleilhavoup, M.; Bertrand, G.; Peters, J. C. *Angew. Chem., Int. Ed.* **2014**, *53*, 8427–8431. (c) Kundu, S.; Li, B.; Kretsch, J.; Herbst-Irmer, R.; Andradá, D. M.; Frenking, G.; Stalke, D.; Roesky, H. W. *Angew. Chem., Int. Ed.* **2017**, *56*, 4219–4223.
- (10) Munz, D.; Chu, J.; Melaimi, M.; Bertrand, G. *Angew. Chem., Int. Ed.* **2016**, *55*, 12886–12890.
- (11) (a) Marion, N.; Díez-González, S.; Nolan, S. P. *Angew. Chem., Int. Ed.* **2007**, *46*, 2988–3000. (b) Fèvre, M.; Pinaud, J.; Gnanou, Y.; Vignolle, J.; Taton, D. *Chem. Soc. Rev.* **2013**, *42*, 2142–2172. (c) Hopkinson, M. N.; Richter, C.; Schedler, M.; Glorius, F. *Nature* **2014**, *510*, 485–496. (d) Naumann, S.; Dove, A. P. *Polym. Chem.* **2015**, *6*, 3185–3200. (e) Flanagan, D. M.; Romanov-Mikhailidis, F.; White, N. A.; Rovis, T. *Chem. Rev.* **2015**, *115*, 9307–9387.
- (12) For selected references: (a) Jana, A.; Huch, V.; Rzepa, H. S.; Scheschkewitz, D. *Organometallics* **2015**, *34*, 2130–2133. (b) Sidiropoulos, A.; Jones, C.; Stasch, A.; Klein, S.; Frenking, G. *Angew. Chem., Int. Ed.* **2009**, *48*, 9701–9704. (c) Ghadwal, R. S.; Roesky, H. W.; Merkel, S.; Henn, J.; Stalke, D. *Angew. Chem., Int. Ed.* **2009**, *48*, 5683–5686. (d) Filippou, A. C.; Chernov, O.; Schnakenburg, G. *Angew. Chem., Int. Ed.* **2009**, *48*, 5687–5690. (e) Filippou, A. C.; Lebedev, Y. N.; Chernov, O.; Straßmann, M.; Schnakenburg, G. *Angew. Chem., Int. Ed.* **2013**, *52*, 6974–6978.
- (13) For selected references: (a) Zhong, R.; Lindhorst, A. C.; Groche, F. J.; Kühn, F. E. *Chem. Rev.* **2017**, *117*, 1970–2058. (b) Ghadwal, R. S.; Azhakar, R.; Roesky, H. W. *Acc. Chem. Res.* **2013**, *46*, 444–456. (c) Bourissou, D.; Guerret, O.; Gabbai, F. P.; Bertrand, G. *Chem. Rev.* **2000**, *100*, 39–91.
- (14) For selected references: (a) Jana, A.; Majumdar, M.; Huch, V.; Zimmer, M.; Scheschkewitz, D. *Dalton Trans.* **2014**, *43*, 5175–5181. (b) Jana, A.; Omlor, I.; Huch, V.; Rzepa, H. S.; Scheschkewitz, D. *Angew. Chem., Int. Ed.* **2014**, *53*, 9953–9956. (c) Jana, A.; Huch, V.; Scheschkewitz, D. *Angew. Chem., Int. Ed.* **2013**, *52*, 12179–12182. (d) Rupar, P. A.; Staroverov, V. N.; Ragogna, P. J.; Baines, K. M. *J. Am. Chem. Soc.* **2007**, *129*, 15138–15139.
- (15) (a) Tomás-Mendivil, E.; Hansmann, M. M.; Weinstein, C. M.; Jazzar, R.; Melaimi, M.; Bertrand, G. *J. Am. Chem. Soc.* **2017**, *139*, 7753–7756. (b) Melaimi, M.; Jazzar, R.; Soleilhavoup, M.; Bertrand, G. *Angew. Chem., Int. Ed.* **2017**, *56*, 10046–10068.
- (16) Bertrand, G.; Lavallo, V.; Canac, Y. WO Patent 2006138166, 2006.
- (17) Paul, U. S. D.; Radius, U. *Chem. - Eur. J.* **2017**, *23*, 3993–4009.
- (18) Alder, R. W.; Blake, M. E.; Chaker, L.; Harvey, J. N.; Paolini, F.; Schütz, J. *Angew. Chem., Int. Ed.* **2004**, *43*, 5896–5911.
- (19) See [Supporting Information](#) for details.
- (20) Jigami, T.; Takimiya, K.; Otsubo, T.; Aso, Y. *J. Org. Chem.* **1998**, *63*, 8865–8872.
- (21) Chilton, N. F.; Anderson, R. P.; Turner, L. D.; Soncini, A.; Murray, K. S. *J. Comput. Chem.* **2013**, *34*, 1164–1175.
- (22) Neese, F. *Orca*, Density Functional and Semiempirical Program Package, 2008; Vol. 2.